SECTION IV

Linacs, Circulating Accelerators, Storage Rings, and Pulsed Power Systems

Particle Accelerators, 1992, Vols. 37–38, pp. 225–233
Reprints available directly from the publisher
Photocopying permitted by license only

NUMERICAL SIMULATION OF HIGH-CURRENT ION BEAM ACCELERATION AND CHARGE COMPENSATION IN MAGNET-ISOLATED SYSTEMS

N. G. BELOVA

Institute of Physics and Technology, USSR Academy of Sciences, 117218 Moscow, USSR

and

V. I. KARAS'

Kharkov Institute of Physics and Technology, Ukrainian SSR Academy of Sciences, 310108 Kharkov, USSR.

(Received 3 December 1990)

Results are reported from the numerical study of processes in the linear high-current induction accelerator. The particle-in-cell method for open systems is used for the simulation. The investigation of dynamics of simultaneous electron and ion beams propagation through an axisymmetric magnet-isolated gap has shown that:

- charge and current compensations occur in the high-current ion beam case in accordance with the recently known mechanism;
- the ion beam is stable for the time essentially greater than the reciprocal ion Langmuir and Larmor frequencies;
- under certain conditions the electric field applied to the gap efficiently accelerates the ion beam particles without disturbing the stability, charge and current compensations of the beam.

1 INTRODUCTION

Several approaches to production of high-current ion beams (with a particle energy $\varepsilon \approx 1$ Gev and $I \approx 10$ KA) by means of an induction accelerator are now being considered for controlled thermonuclear fusion research[1].

The present-day linear high-current induction accelerators (linacs) with magnet-isolated accelerating gaps can provide kiloampere ion beams with an energy of several hundred keV[2–5]. Since the power and brightness requirements for ion beams in controlled thermonuclear fusion research are very stringent, a number of important physical problems (discussed in Ref. 6) must be studied in order to develop a driver for controlled thermonuclear fusion based on a high-current linac.

One of the approaches to production of a charge-compensated high-current ion beam in a magnet-isolated accelerating gap is to attain synchronous transport of equally dense electron and ion beams through the gap as a result of electron drift. Since the axisymmetric configuration cannot provide the azimuthal electric polarization field, (hence the electron drift)[7,8], a new mechanism has been proposed in[9] for compensating the high-current ion beam in a magnet-isolated accelerating gap (cusp). Its physical meaning is that a specially injected neutralizing electron beam drifts through the cusp due to both the self-consistent magnetic field B_θ and the electric field E_r produced by a small radial separation of the ion and electron beams.

An analytic treatment based on the hydrodynamical description of the electron beam and on Maxwell's equations for B_θ and E_r has made it possible to specify the required parameters of the electron and ion beams[9,10]. The required particle energy in the electron beam, ε_0, is considerably less than the energy required for the electrons to overcome the magnetic isolation, but is greater than the energy spent to overcome potential differences in the accelerating gap:

$$eE_0 L < \varepsilon_0 \ll \frac{e^2 \mathbf{B}_0^2 L^2}{2m_e c^2}, \tag{1}$$

$$n_i > \frac{\mathbf{B}^2}{4\pi m_e c^2}, \quad \Delta \geq \frac{c\Omega_s}{\omega_s^2}. \tag{2}$$

Here, E_0 is the external accelerating electric field: $\mathbf{B}_0$ is the amplitude of the external magnetic field; L is the characteristic length of the accelerating gap, $\Omega_s = (e\mathbf{B}_0/m_s c)$; $\omega_s^2 = (4\pi e^2 n_s/m_s)$; Δ is the beam thickness; m_s and n_s are the rest mass and the density of the particles of type s ($s = e, i$); and c is the speed of light.

Condition (2) means that the transported ion beam must have a rather high current.

Here we present the results of our numerical investigation of electron and ion beams dynamics in a magnet-isolated accelerating gap. The computer simulation is performed with the help of the particle-in-cell (PIC) model[11,12] for the open plasma configuration, in particular for spatially bounded systems with injection and escape of electrons and ions[13,14]. A number of papers have been devoted to numerical simulations of collisionless processes in axisymmetric systems by the PIC method (see Refs. [15–18] and the literature cited there).

2 BASIC EQUATIONS AND BOUNDARY CONDITIONS

To describe the dynamics of a collisionless plasma in both the self-consistent and the external electromagnetic fields in axisymmetric ($\partial/\partial\theta = 0$) geometry, we use the set of relativistic Vlasov's equations for the distribution functions of the given type of particles:

$$\frac{\partial f_s}{\partial t} + \mathbf{v}\frac{\partial f_s}{\partial \mathbf{r}} + \frac{d\mathbf{p}}{dt}\frac{\partial f_s}{\partial \mathbf{p}} = 0, \tag{3}$$

where $\mathbf{p} = m_0\mathbf{v}\gamma$, $\mathbf{v} = \{\dot{r}, r\dot{\theta}, \dot{z}\}$, $\gamma = [1 - (|\mathbf{v}|/c)^2]^{-1/2}$.

The self-consistent electromagnetic fields in Equation (3) are determined by Maxwell's equations, which in the Lorentz gauge (div $\mathbf{A} + (1/c)(\partial\phi/\partial t) = 0$) take the form of wave equations for the dimensionless scalar ϕ and vector $\mathbf{A}$ potentials:

$$0A^i = -4\pi J^i,$$

where $A^i = \{\phi, \mathbf{A}\}$, $J^i = \{\rho, \mathbf{J}\}$, 0 is the d'Alembertian,

$$\rho = \sum_s \int q_s f_s(\mathbf{p}) d\mathbf{p},$$

and

$$J = \sum_s \int q_s \mathbf{v} f_s(\mathbf{p}) d\mathbf{p}.$$

The dimensions of the quantities involved in these equations are defined as follows:

$$\begin{aligned}
[v] &= c;\\
[r, z] &= \mathrm{c}/\omega_{pe};\\
[t] &= \omega_{pe}^{-1};\\
[n] &= n_{oe};\\
[q] &= e;\\
[m] &= m_0;\\
[\phi, A] &= \mathscr{E}_{ch}/e;\\
[E, B] &= (4\pi n_{oe}\mathscr{E}_{ch})^{1/2};\\
[J] &= en_{oe}c;\\
[P_\theta] &= [\psi] = c^2/\omega_{pe},
\end{aligned}$$

where $\omega_{pe} = (4\pi n_{oe}e^2/m_0)^{1/2}$ is the electron plasma frequency, $\mathscr{E}_{\mathrm{ch}} = m_0c^2$ is the rest energy of the electron, n_{oe}, m_0, e are the initial density, rest mass and charge of the electrons, respectively, and γ is the relativistic factor.

The equations of motion, obtained as characteristic equations of (3), have the form:

$$\frac{du_r}{dt} = \frac{1}{\gamma}\frac{q}{m}\left[\frac{\psi}{r^2}\frac{\partial}{\partial r}(rA_\theta) - \gamma\frac{\partial A_r}{\partial t} - u_z\left(\frac{\partial A_r}{\partial z} - \frac{\partial A_z}{\partial r}\right)\right] - \frac{q}{m}\frac{\partial\phi}{\partial r} + \frac{1}{\gamma}\frac{\psi^2}{r^3} \tag{5a}$$

$$\frac{du_z}{dt} = \frac{1}{\gamma}\frac{q}{m}\left[\frac{\psi}{r^2}\frac{\partial}{\partial z}(rA_\theta) - \gamma\frac{\partial A_z}{\partial t} + u_r\left(\frac{\partial A_r}{\partial z} - \frac{\partial A_z}{\partial r}\right)\right] - \frac{q}{m}\frac{\partial\phi}{\partial z}, \tag{5b}$$

where $\mathbf{u} = \gamma\mathbf{v}$, $\psi = \gamma r^2\dot{\theta} = P_\theta - (q/m)rA_\theta$ (P_θ is the dimensionless generalized particle momentum), and

$$\gamma = \left[1 + u_r^2 + \left(\frac{\psi}{r}\right)^2 + u_z^2\right]^{1/2}.$$

The dimensionless system of Equations (3)–(5) is closed by the boundary and initial conditions.

The boundary conditions for the distribution functions at ($z = 0, z = z_L$) set the injection regime:

$$f_s(\mathbf{p}, \mathbf{R}, t)|_{z=0} = \begin{cases} f_s(\mathbf{p}, r, 0, t), r_{\min} \le r \le r_{\max} \\ 0, 0 \le r < r_{\min}, r_{\max} < r \le r_L \end{cases}, \; p_z > 0,$$
$$f_s(\mathbf{p}, \mathbf{R}, t)|_{z=z_L} = \begin{cases} f_s(\mathbf{p}, r, z_L, t), r_{\min} \le r \le r_{\max} \\ 0, 0 \le r < r_{\min}, r_{\max} < r \le r_L \end{cases}, \; p_z < 0, \tag{6}$$

and at ($r = 0, r = r_L$) set the reflection regime:

$$f_s(\mathbf{p}, \mathbf{R}, t)|_{r=0,\, r_L} = f_s(-p_r, p_z, p_\theta, \mathbf{R}, t), \; z \subset [0, z_L]. \tag{7}$$

At the initial time, the distribution functions are equal to

$$f_s(\mathbf{p}, \mathbf{R}, 0) = f_{os}(\mathbf{p}, \mathbf{R}), \; z \subset [0, z_L], \; r \subset [0, r_L],$$
$$\mathbf{R} = \{r, z\}. \tag{8}$$

The boundary conditions for the potentials are

$$r = 0\text{: } \partial\phi/\partial r = 0, \; \partial A_z/\partial r = A_r = \partial A_\theta/\partial r = 0;$$
$$r = r_L\text{: } \phi = \phi(z), \; A_z = A_r = A_\theta = 0; \tag{9}$$
$$\left.\begin{matrix} z = 0 \\ z = z_L \end{matrix} : \begin{matrix} \phi = \phi_0 \\ \phi = \phi_L \end{matrix}\right\}, \; \partial A_z/\partial z = -(1/r)\frac{\partial}{\partial r}(rA_r), \; \partial A_r/\partial z = \partial A_\theta/\partial z = 0.$$

The method and algorithm of the solution of (3)–(5) are described in Refs. [17,18].

The above model was carried out as a 2,5-dimensional cylindrical code (with the phase coordinates of particles $-r$, z, v_r, v_z, P_θ) for the ES, VAX, and IBM-PC computers. Up to three types of particles can be considered in the calculations. The greatest possible number of particles may be 600 000 for the given program structure.

3 RESULTS OF THE NUMERICAL INVESTIGATION OF THE PROPAGATION DYNAMICS OF ELECTRON AND ION BEAMS THROUGH A CUSP

Let a hollow magnetized electron beam with velocity V_e and a hollow unmagnetized ion beam with velocity V_i be injected along the z axis into the external magnetic field defined by the function $A_\theta = -(\mathbf{B}_0/k) \cdot I_1(kr) \cdot \cos(kz)$, where $I_1(kr)$ is the first-order

modified Bessel function. The beam current densities are equal to $q_e n_{oe} V_e = q_i n_{oi} V_i$. The dimensionless equations for solving this problem have the form of Eqs. (3)–(5) with the initial and boundary conditions from Eqs. (6)–(9), where

$$f_s(\mathbf{p}, r, 0, t) = \delta(u_r)\delta(u_z - u_{os})\delta(u_\theta),\ f_s(\mathbf{p}, r, z_L, t) = 0,$$

$$f_{os}(\mathbf{p}, \mathbf{R}) = 0,\ u_{oe} = V_e/(1 - V_e^2)^{1/2},\ u_{oi} = V_i/(1 - V_i^2)^{1/2},$$

and

$$u_\theta = r\dot{\theta} = P_\theta - (q_s/m_{os})rA_\theta = 0;$$

$$\phi(z) = \begin{cases} 0, & 0 \le z \le \Delta_z, \\ (k-1)\cdot\Delta_\phi + \dfrac{\Delta_\phi}{\Delta_z}[z - (2k-1)\cdot\Delta_z], & (2k-1)\cdot\Delta_z \le z \le 2k\cdot\Delta_z, \\ k\cdot\Delta_\phi, & 2k \le z \le (2k+1)\cdot\Delta_z, \end{cases}$$

$\Delta_\phi = (\phi_L - \phi_0)/\mathcal{K}$, $\Delta_z = z_L/(2\mathcal{K} + 1)$, $k = 1, \ldots, \mathcal{K}$, $\mathcal{K}$ is the total number of cusps, and $k = \mathcal{K}\pi/z_L$.

The initial conditions for the self-consistent fields are

$$\phi = A_z = A_r = A_\theta = 0.$$

In the calculations we assumed the mass ratio to be $m_i/m_e = 100$; $m_e = 20m_0$; and the number and velocity of particles in the cell were $N_e = 64$, $N_i = 180$, $V_e = 0.8$ $V_i = 0.285$. Four variants were run with the following dimensionless parameters:

N	r_L	z_L	$r_{\max}$	$r_{\min}$	$\mathbf{B}_0$	Δt	$\Delta\tau$	Δ_ϕ	$\mathcal{K}$
1	15.875	7.875	3.25	3.0	17.6	0.025	0.0125	0	1
2	157.5	78.75	32.5	30.0	1.76	0.01	0.005	0	1
3	157.5	78.75	32.5	30.0	1.76	0.05	0.025	1	1
4	157.5	78.75	35.0	25.0	1.76	0.05	0.025	5	2

The number of points for solving Maxwell's equations was (32 × 64) in the first variant and (64 × 64) in the remaining cases.

The results of the calculations are shown for case 1 (Figure 1), case 2 (Figure 2) and case 3 (Figures 3 and 4).

It is seen from Figure 1 that the ion beam is partially neutralized by the electrons only in the first half of the cusp (parts a and b): therefore, the total charge density grows rapidly in the second half of the cusp, getting positive and large (part b). There is also no compensation of the B_θ field (part c), and a sharp positive peak of the scalar potential ϕ (part d) is observed in the second half of the region. The electron beam particles oscillate in the first half of the cusp (part a).

Figure 2 demonstrates the steady-state drift of the electron beam through the magnet-isolated gap (parts a and b). The total charge density of macroparticles $\rho(r, z)$ is considerably lower in the second half of the cusp (part b) than in Case 1. This is due

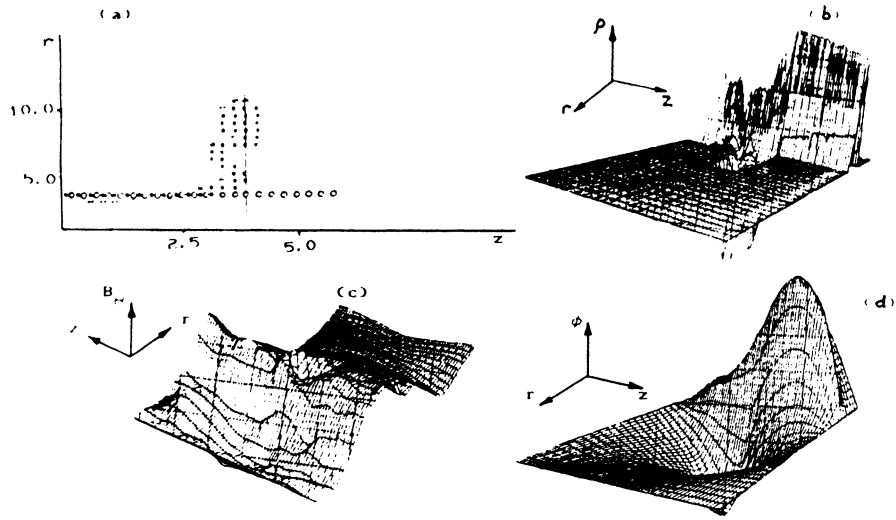

FIGURE 1 Distributions of the following:
(a) electrons (stars) and ions (circles) on the r, z plane; $t = 24.5$.
(b) total charge density $\rho(r, z)$.
(c) azimuthal magnetic field $B_\theta(r, z)$.
(d) scalar potential $\phi(r, z)$ after passage of the ion beam through the entire region.

Here, $t = 39$, $\rho_{\max} = 2.7$, $\rho_{\min} = -2.2$, $B_{\theta\max} = 0.56$, $B_{\theta\min} = -0.11$, $\phi_{\max} = 1.3$, $\phi_{\min} = -0.8$.

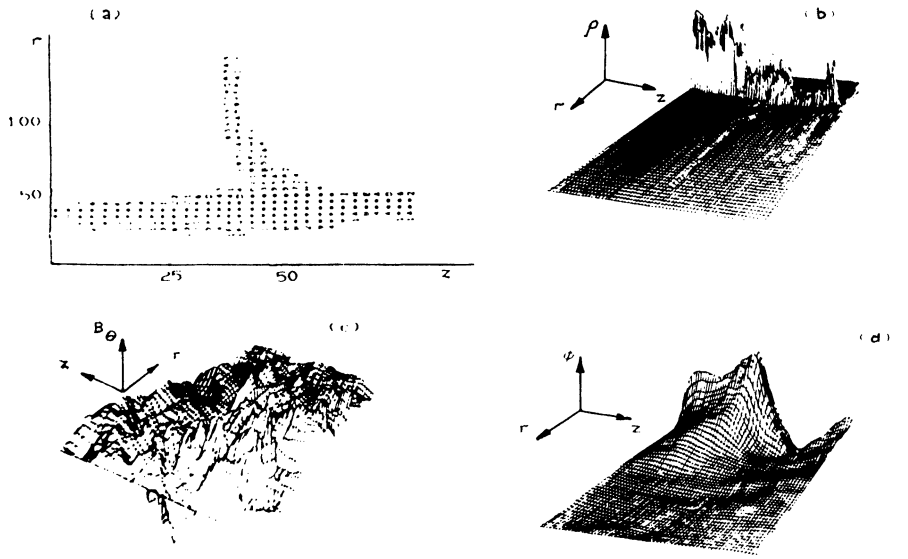

FIGURE 2 Distributions of the following:
(a) electrons (stars) on the r, z plane, $t = 275$.
(b) total charge density $\rho(r, z)$.
(c) azimuthal magnetic field $B_\theta(r, z)$.
(d) scalar potential $\phi(r, z)$ after passage of the ion beam through the entire region.

Here, $t = 225$, $\rho_{\max} = 1.2$, $\rho_{\min} = -1$, $B_{\theta\max} = 1.5$, $B_{\theta\min} = -1.5$, $\phi_{\max} = 24.8$, and $\phi_{\min} = -13.4$.

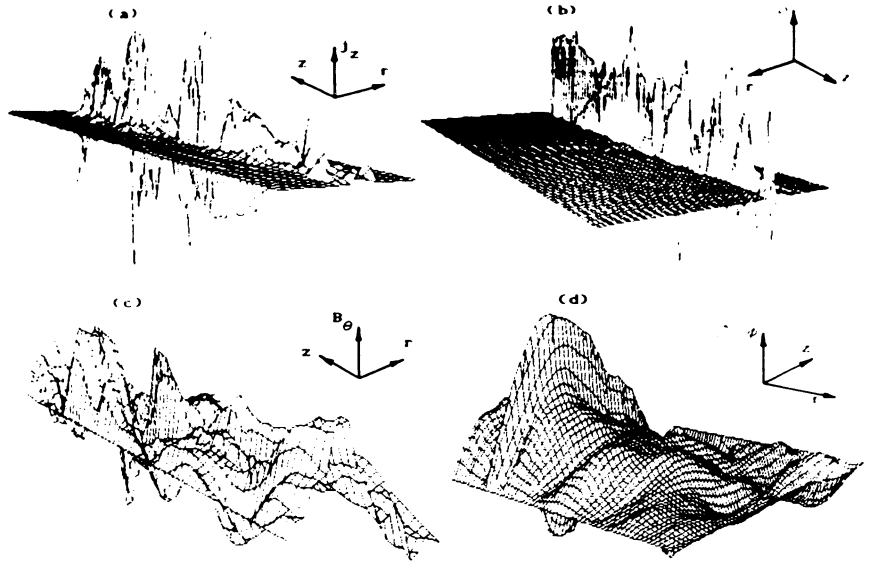

FIGURE 3 Distributions of the following:
(a) total axial current density $j_z(r, z)$.
(b) total charge density $\rho(r, z)$.
(c) azimuthal magnetic field $B_\theta(r, z)$.
(d) scalar potential $\phi(r, z)$ after passage of the ion beam through the entire region.

Here, $t = 340, j_{z\max} = 0.7, j_{z\min} = -1.1, \rho_{\max} = 2.1, \rho_{\min} = -1.7, B_{\theta\max} = 5.5, B_{\theta\min} = -4.3,$ $\phi_{\max} = 15.8,$ and $\phi_{\min} = -16.$

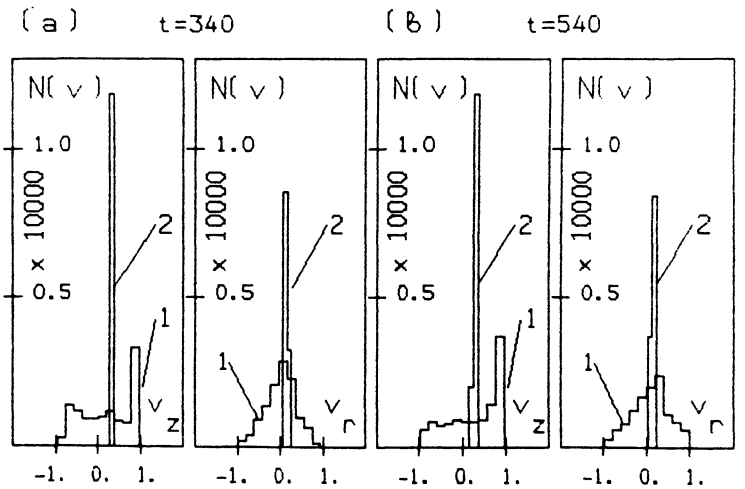

FIGURE 4 Distribution functions N(V) of the (1) electron and (2) ion beams versus the longitudinal (V_z) and transverse (V_r) velocities at $t = 340$ (a) and $t = 540$ (b).

to charge neutralization of the ion beam by electrons. This is also evident from the distribution $B_\theta(r, z)$ and $\phi(r, z)$ (parts c and d).

The distributions of the functions $J_z(r, z)$ (part a), $\rho(r, z)$ (part b), $B_\theta(r, z)$ (part c) and $\phi(r, z)$ (part d), presented in Figure 3, show that the applied external electric field, which accelerates ions and retards electrons, does not disrupt the electron beam drift through the accelerating gap. From the functions $J_z(r, z)$ (part a) and $B_\theta(r, z)$ (part c), it is clearly seen that not only charge compensation (parts b and d) but also current compensation of the ion beam occurs.

Figures 4a and 4b show the distribution functions N(V) of the electron (1) and ion (2) beams versus the longitudinal (V_z) and transverse (V_r) velocities at $t = 340$ and $t = 580$, respectively. It is seen that the ion beam generally retains a monoenergetic shape, because its spread in V_z and V_r does not exceed 10%. The electron beam spread in the velocities is nearly 100%, but this does not prevent charge compensation of the ion beam by electrons.

Case 4 corresponds to the rather wide electron and ion beams and to a high accelerating electric field applied to two magnet-isolated gaps. In this case, the charge neutralized ion beam is transported because of the electron beam drift through the two cusps. However, to produce an ion beam of the required quality, it is necessary to continue the optimization of the system parameters.

4 DISCUSSION OF THE RESULTS

The simulation parameters of variant 1 correspond to a rather low-current ion beam whose parameters do not satisfy Eq. (2). Cases 2, 3, and 4 correspond to the case of the high-current ion beam; Eq. (2) is satisfied, i.e., the condition of ion beam passage through a magnet-isolated gap owing to the electron drift is fulfilled. This demonstrates the possibility of the compensated ion beam transport through a magnet-isolated gap.

Let us apply the above results of the computer simulations to the real model of a high-current linac[3]. The length of the accelerating gap is $L \approx 5$ cm, the radius of the chamber is $R \approx 10$ cm, the characteristic magnetic field value is $B_0 \approx 7.5$ kG, the Larmor radius of electrons is $r_{Le} \approx 0.045$ cm ($r_{Le} \ll L$), and the Larmor radius of ions is $r_{Li} \approx 20$ cm ($r_{Li} \gg L$). Case 1 corresponds to the electron beam density $n_{oe} = 8 \cdot 10^{11}$ cm^{-3}, and Cases 2, 3, and 4 correspond to $n_{oe} = 8 \cdot 10^{13}$ cm^{-3}. Thus, high-current ion beams can be accelerated in the linac with a substantial space-charge compensation within the magnet-isolated gaps.

The authors are grateful to Prof. Ya. B. Fainberg for his constant interest to this work and useful discussions.

REFERENCES

1. A. Faltens and D. Keefe, in *Proceedings of the 1981 Linear Accelerator Conference, (Santa Fe, New Mexico, 1982)* LA-9234c, p. 205.
2. A. I. Morozov and S. V. Lebedev, in *Reviews of Plasma Physics* **8**, edited by M. A. Leontovich (Consultants, New York, 1980), p. 247.

3. V. A. Kiyashko, Yu. E. Kolyada, E. A. Kornilov, and Ya. B. Fainberg, *Pis'ma Zh. Tekh. Fiz.* **3**, 1257 (1977) [*Sov. Tech. Phys. Lett.*, **3**, 519 (1977)].
4. S. Humphries, Jr., *Nucl. Fusion*, **20**, 1549 (1980).
5. I. S. Roth, J. D. Ivers, and J. A. Nation, in Proceedings of the Sixth International Conference on High Power Particle Beams, Kobe, (1986), p. 689.
6. V. I. Karas', V. A. Kiyashko, E. A. Kornilov, Ya. B. Fainberg, *Nucl. Instrum. Meth. A* **278**, 245 (1989).
7. K. D. Sinel'nikov and B. N. Rutkevich, *Zh. Tekh. Fiz.* **37**, 56 (1967) [*Sov. Phys. Tech.* **12**, 37 (1967)].
8. W. Peter, N. Rostoker, *Phys. Fluids* **22**, 730 (1982).
9. V. I. Karas', V. V. Mukhin, V. E. Novikov, and A. M. Naboka, *Fiz. Plazmy* **13**, 494 (1987) [*Sov. J. Plasma Phys.* **13**, 281 (1987)].
10. V. I. Karas', V. V. Mukhin, and A. M. Naboka, in *Proceedings of the Fourth International Workshop on Nonlinear Processes in Physics*, Kiev (1989), p. 329.
11. Yu. S. Sigov, *Numerical Methods in the Kinetic Theory of Plasmas* [Russian] (MFTI, Moscow, 1984).
12. R. Hockney and J. Eastwood, *Computer Simulation Using Particles*, (McGraw-Hill, London, 1981).
13. Yu. S. Sigov, *Physica Scripta* **2**, 367 (1982).
14. N. G. Belova and Yu. S. Sigov, Preprint No. 69, IPM AN SSSR, Moscow (1982).
15. J. Killeen and S. L. Rompel, *J. Comp. Phys.* **1**, 29 (1966).
16. M. Brettschneider and J. Killeen, *J. Comp. Phys.* **11**, 360 (1973).
17. N. G. Belova and Yu. S. Sigov, Preprint No. 30, IPM AN SSSR, Moscow (1989).
18. N. G. Belova, V. I. Karas' and Yu. S. Sigov, *Fiz. Plazmy* **16**, 209 (1990) [*Sov. J. Plasma Phys.* **16**, 115 (1990)].